ResearchGate

See discussions, stats, and author profiles for this publication at: https://www.researchgate.net/publication/236888532

Reaction Mechanisms of Water Splitting and H2 Evolution by a Ru(II)−Pincer Complex Identified with Ab Initio Metadynamics Simulations

ARTICLE *in* ACS CATALYSIS · JULY 2012

Impact Factor: 9.31 · DOI: 10.1021/cs300350b

CITATIONS
5

READS
32

3 AUTHORS:

Changru Ma
École Polytechnique Fédérale de Lausanne
7 PUBLICATIONS **11** CITATIONS
SEE PROFILE

Simone Piccinin
Italian National Research Council
42 PUBLICATIONS **435** CITATIONS
SEE PROFILE

Stefano Fabris
Italian National Research Council
75 PUBLICATIONS **6,247** CITATIONS
SEE PROFILE

Available from: Simone Piccinin
Retrieved on: 26 January 2016

ACS Catalysis

Research Article

pubs.acs.org/acscatalysis

Reaction Mechanisms of Water Splitting and H_2 Evolution by a Ru(II)-Pincer Complex Identified with Ab Initio Metadynamics Simulations

Changru Ma,[†] Simone Piccinin,[‡,†] and Stefano Fabris*[,‡,†,§]

[†]SISSA, Scuola Internazionale Superiore degli Studi Avanzati, Via Bonomea 265, 34136 Trieste, Italy

[‡]CNR-IOM, DEMOCRITOS Simulation Center, Istituto Officina dei Materiali, c/o SISSA, Via Bonomea 265, 34136 Trieste, Italy

[§]IIT-SISSA Unit, Italian Institute of Technology, Via Bonomea 265, 34136 Trieste, Italy

Supporting Information

ABSTRACT: Water splitting is at the basis of artificial photosynthesis for solar energy conversion into chemical fuels. While the oxidation of water to molecular oxygen and the reduction of protons to molecular hydrogen are typically promoted by different catalysts, the Ru(II)-pincer complex recently synthesized by Kohl et al. [*Science* **2009**, *324*, 74] has been shown to promote both the thermal driven formation of H_2 and the UV−vis driven evolution of O_2. Here, we investigate, through density functional theory calculations, a portion of the catalytic cycle, focusing on the formation of hydrogen. We adopt an explicit description of the solvent and employ metadynamics coupled with the Car−Parrinello method to study the reaction mechanism and determine the activation free energies. Our simulations predict a novel catalytic cycle, which has considerably lower activation energies than earlier proposals and which does not involve the sequential aromatization−dearomatization of the PNN ligand of the complex. This work clearly demonstrates the general importance of an explicit description of the solvent for a predictive modeling of chemical reactions that involve the active participation of the solvent.

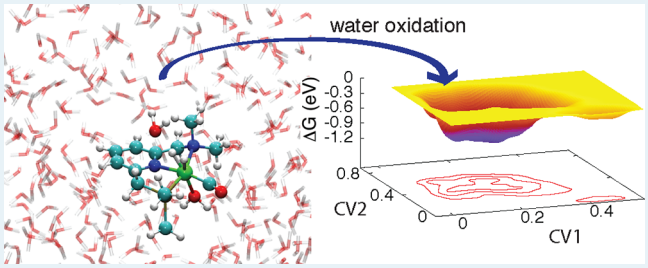

KEYWORDS: *homogenous catalysis, water splitting, modeling reaction mechanisms in solution, density functional theory and metadynamics, Ru(II)-pincer complex*

1. INTRODUCTION

The sunlight-driven splitting of water into H_2 and O_2 is a milestone for storing solar energy in chemical fuels.[1−3] This electrochemical reaction involves two semireactions: water oxidation at the anode, releasing protons and evolving O_2; and reduction of protons at the cathode, evolving H_2. Among these, the water oxidation semireaction is by far the most challenging and represents a bottleneck for the development of efficient artificial photosynthesis devices for the production of solar fuels.[4−6]

Although most of the molecular catalysts promoting efficient water oxidation comprise cores containing multiple metal centers,[7−10] some single-center complexes have also been reported.[11−15] Among these, the recent discovery and characterization of a Ru(II)-pincer is of fundamental importance since it demonstrates that a single metal center can promote the whole reaction, namely, water oxidation as well as H_2 evolution.[14] Full characterization of the reaction mechanism of this homogeneous catalyst would have important fundamental and technological implications. Ab initio simulations have already provided useful information toward this characterization, proposing several possible reaction paths for the thermal- and light-driven H_2 and O_2 evolutions, respectively.[16−19]

This Ru(II)-pincer complex (P-da-PNN)RuH(CO) (**0**, P-da = dearomatized at the phosphorus side arm, PNN = (2-(di-*tert*-butylphosphinomethyl)-6-diethylaminomethyl)pyridine) in a tetrahydrofuran aqueous solution activates a water molecule by forming a *trans*-hydrido-hydroxo complex, which yields aromatization of the PNN ligand.[14] Heating at 100 °C releases H_2 with concomitant formation of a *cis*-dihydroxo intermediate. Upon irradiation with 320−420 nm UV−vis light, O_2 is evolved, probably by first liberating H_2O_2, which then catalytically disproportionates to O_2 and water.[14]

The solvent plays a key role in the function of water-oxidation catalysts and introduces significant complexities into the simulations, which often relies on simplified solvent models. In particular, previous simulations have captured the electrostatic effects of the solvent on the reaction sites/intermediates through implicit solvent descriptions. This is a very powerful and popular technique, which has, however, one important limitation. It precludes/limits the exchange of products, reactants, and intermediates between the solvent and the reaction sites, essentially preventing the active participation of the solvent in the reaction. In this paper, we demonstrate the importance of describing explicitly the solvent for simulating

Received: June 5, 2012
Published: June 11, 2012

 © 2012 American Chemical Society dx.doi.org/10.1021/cs300350b | *ACS Catal.* 2012, 2, 1500−1506

the catalytic function of this Ru-pincer complex. On this basis, we propose a new catalytic cycle for the H−H bond formation at the mononuclear Ru(II)-pincer complex, resulting in lower activation energies than previously proposed cycles.

2. COMPUTATIONAL METHODS

DFT Electronic Structure. The electronic structure is computed using density functional theory (DFT)[20] calculations, employing the Perdew−Burke−Ernzerhof (PBE) generalized gradient approximation (GGA)[21] for the exchange and correlation functional. We use a plane wave ultrasoft-pseudopotentials[22] approach as implemented in the Quantum ESPRESSO package.[23] Kinetic energy cutoffs used to represent the electron wave function and density are 29 and 232 Ry, respectively. All the structures are fully relaxed until the forces on all atoms are below 5×10^{-4} a.u. (0.026 eV/Å). Tests show that spin-polarized calculations converge to singlet ground states for all intermediates, and in all cases, the Ru center carries no spin. All calculations reported in this work are therefore non-spin-polarized.

Structural Model. To reduce the computational cost of the calculations, we apply the same structural simplifications of the catalyst suggested by Kohl et al.,[14] which consist of replacing the P^tBu_2 and NEt_2 groups with PMe_2 and NMe_2 groups (i.e., methyl groups are replaced by hydrogen atoms). We have checked that this approximation has very limited effects on the calculated atomistic and electronic structures as well as on the energetics of the systems under analysis (see the Supporting Information (SI), Figure S1).

Molecular Dynamics in Solution. Car−Parrinello (CP) molecular dynamics (MD) simulations[24] are used to sample the trajectories of the reaction intermediates at finite temperature in water solution. We use a cubic periodic supercell containing the Ru complex solvated by 73 explicit water molecules. The dimensions of the cubic box (L = 25.188 au) are determined with a preliminary classical MD simulation of ≈1 ns in the NPT ensemble at zero pressure. Here, water is described with the TIP3P model,[25] and the interaction between water and the Ru complex is described through a Lennard-Jones potential combined with the Coulomb interaction among point charges. This classical simulation is followed by an ab initio CP MD equilibration run of ≈15 ps in the NVT ensemble, where we apply the Nosé−Hoover thermostat.[26] All our CP simulations employ a fictitious mass of 350 a.u. and an integration time step of 3 a.u. (0.073 fs), which ensures adiabatic decoupling between the electronic and ionic motion.

Metadynamics and Reaction Free Energy. Reaction mechanisms and the corresponding free energy surfaces are studied with the metadynamics technique[27] using the PLUMED plug-in[28] interfaced with the Quantum ESPRESSO package. Details of this technique and of the collective variables (CV) used to follow the reaction are described in the following and in the SI (eq 4). Note that these simulations are used to predict the reaction mechanism with the minimum activation free energy. The simulations are stopped when the system overcomes this minimum-energy barrier and reaches the final state. The final state basin is not sampled, and hence, free energy differences between initial and final states are not computed. To increase the accuracy of the calculated activation energy for the rate-limiting step (H_2 formation step), we repeat the calculation three times and average the resulting activation free energy. Further details of the simulation parameters used in the metadynamics simulations are given in the Supporting Information.

3. RESULTS AND DISCUSSIONS

To validate our computational approach, we first performed a preliminary analysis of the Ru complex in gas phase along the reaction mechanisms for water oxidation and H_2 formation at the Ru center proposed in the earlier DFT simulations.[16,17] Our results are in good agreement with these data, particularly concerning the molecular and electronic structures, and the energy barriers between the reaction intermediates (see the section entitled "Preliminary analysis in gas phase" in the SI). We therefore support the same conclusions about the reaction paths identified in vacuum. In particular, a full structural characterization (main bond lengths and angles) of the key intermediates both in gas phase and in explicit solution is reported in SI Tables S1, S2, and S3. This analysis shows that there is no significant effect of the solvent on the intramolecular distances.

To investigate the solvent effects on these reaction mechanisms, we take an approach that is different from previous computational works. Instead of performing single-point calculations on the gas-phase optimized structures by including a polarizable continuum model for water, we describe the solvent explicitly at the quantum level, thus allowing its participation in the reaction. CP MD and metadynamics are used to predict novel possible reaction mechanisms and catalytic cycles.

3.1. Catalyst Solvation. The measurements of Kohl et al.[14] show that the interaction of the Ru complex **0** with a water molecule yields aromatization of the PNN ligand and leads to complex **1** (**0** → **1**, Scheme 1). This is suggested to be the

Scheme 1. Reaction of Water with Complex 0

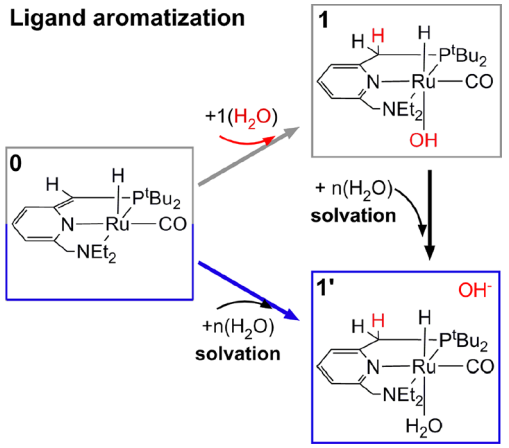

configuration of the catalyst promoting the thermal formation of H_2. The PNN ligand aromatization is proposed to be a consequence of water binding and dissociation at the under-coordinated Ru center, which drives the formation of a hydroxo ligand at the Ru vacant site and H saturation of the sp^2 C1 site of the PNN ligand. Solvating complex **1** in water and heating lead to H_2 evolution.

To fully characterize the solvation of catalyst **1**, its vacuum-optimized molecular configuration is solvated with 73 water molecules described at the quantum level. The dynamics of the process is simulated with CP MD at room T for 18.2 ps. This simulation shows that in water solution, the hydroxo ligand of **1**

dx.doi.org/10.1021/cs300350b | ACS Catal. 2012, 2, 1500−1506

is not stable. Within the first 3 fs, the hydroxo ligand activates a proton transfer from a neighboring solvent water molecule, leading to a H_2O ligand and a hydroxide in solution (**1** → **1′** in Figure 1; additional details in SI Figure S4).

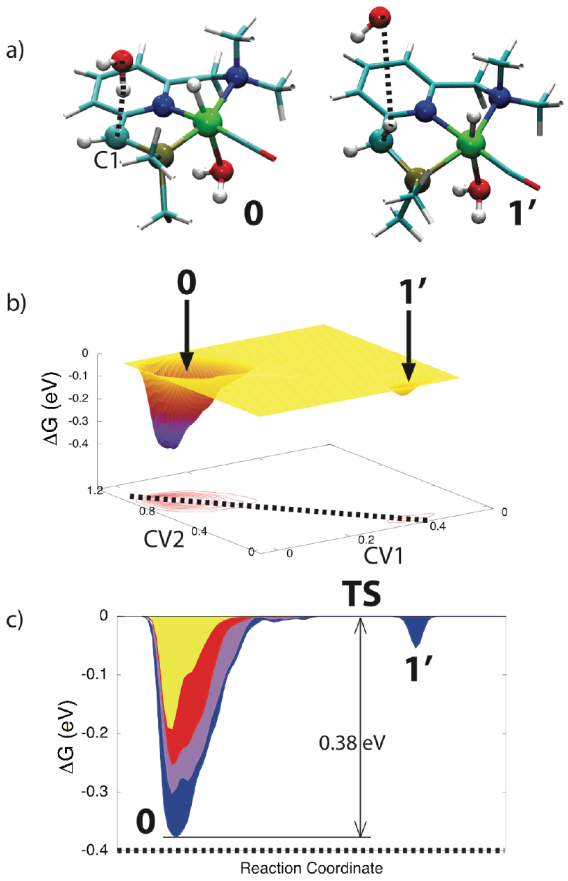

Figure 1. Reaction mechanism for the PNN ligand aromatization. (a) Representative configurations of the initial (**0**) and final (**1′**) states taken from snapshots of the metadynamics simulations. (b) Free energy surface as a function of the CVs defined as the coordination numbers between C1 and H (CV1) and between O and H (CV2). (c) 2D cut of the free energy surface between **0** and **1′**. The activation energy is 0.38 eV. Green, blue, tan, cyan, white, and red spheres represent Ru, N, P, C, H, and O atoms, respectively. The solvent water molecules are not shown.

Repeating the simulation with several different initial configurations always led to the same final result: namely, the formation of a water ligand in place of the hydroxo one. The result is also invariant with respect to the size of the simulation box and the concentration of the solution (i.e., the number of solvent water molecules in the simulation). We solvated complex **1** with 202 water molecules in a cubic box with a lateral dimension of 34.73 au, still finding that, within a few femtoseconds, complex **1** converts into complex **1′** (see the SI). The protonation of complex **1** in solution is further clarified by the Löwdin charge analysis reported in Table S5 (SI). The total charge of the system increases by ∼1*e* during the **1** → **1′** transformation. At the same time, the charge of the Ru does not change significantly. It can therefore be concluded that, indeed, a proton is transferred from the solvent to the OH ligand of complex **1** and that this protonation does not modify the oxidation state of the Ru(II) center. Note that the use of an implicit solvent model would have artificially suppressed the spontaneous OH → H_2O ligand conversion via proton transfer from the solvent.

This surprising result points to an alternative route for the aromatization of the PNN ligand that we address in the following. Moreover, it also suggests that **1′**, instead of **1**, could be the relevant catalyst for H_2 formation. Before addressing the reaction mechanism, we investigate whether **1′** may originate from the solvation of **0** (**0** → **1′** in Scheme 1 and Figure 1).

3.2. Solvent Induced Aromatization of PNN Ligand.

Here, we address the ligand aromatization mechanism for complex **0** in water solution. We note that in the experiment,[14] the aromatization of the PNN ligand occurs in a solution of tetrahydrofuran with the addition of 1 equiv of water. The system is then exposed to refluxing water for several hours, and evolution of molecular H_2 is observed. We approximate this final solvent with pure water, thus neglecting the role of the tetrahydrofuran molecules. We expect that this approximation has no major effects on the aromatization process.

The stable molecular configuration of **0** in water is determined by CP MD simulations, in which the vacuum-optimized molecular configuration of **0** is solvated and equilibrated in a NVT ensemble for 10 ps. These simulations show that a water molecule binds to the under-coordinated Ru center, opposite to the H ligand, within the first 11 fs of the simulation. Ligand aromatization has been suggested to proceed via splitting of this ligated water, followed by proton migration to the unsaturated carbon atom (C1) of the PNN ligand, and formation of a Ru-hydroxo ligand (complex **1**). Having shown that complex **1** is unstable in water and readily converts to **1′**, here we explore a different mechanism for PNN ligand aromatization involving the splitting of a solvent water molecule close to and activated by the C1 site (Figure 1a).

We explored this alternative reaction path through metadynamics simulations biasing two collective variables: (CV1) the coordination number of C1 with respect to the hydrogen of the nearest solvent water molecule and (CV2) the coordination number of this hydrogen with respect to the oxygen in the water molecule (additional calculation details are in the SI). The free energy surface resulting from biasing these two CVs is shown in Figure 1b). The deep energy minimum in the CV domain corresponds to the initial state, solvated **0**, Figure 1a). The first transition occurring in the metadynamics run is the one with the lowest activation energy and leads to the **1′** complex. Quite importantly, this final state is consistent with the one resulting from the solvation of complex **1**, described above. The process leads to a hydroxide in solution that quickly diffuses away from the catalyst.

The free-energy two-dimensional section connecting the initial and final states is shown in Figure 1c). The simulations predict an activation energy for the **0** → **1′** transition of 0.38 eV. This energy barrier turns out to be comparable to the previously calculated ones for the **0** → **1** transition, 0.33–0.13 eV.[16,17] Differences between these energy barriers are clearly within the error bars of the different simulation approaches. Our calculations demonstrate that the ligand aromatization step does not necessarily involve the catalytic action of the Ru center. Given the higher stability of the water ligand compared with the hydroxo ligand at the Ru center, it should not be surprising that the water that dissociates is a solvent molecule rather than the ligated one. Finally, these simulations show that the thermal-activated H–H bond formation is activated by **1′**, instead of by **1**. Quite importantly, the Löwdin charge analysis (SI Table S5) shows that the charge

dx.doi.org/10.1021/cs300350b | *ACS Catal.* 2012, 2, 1500–1506

Scheme 2. Proposed Catalytic Cycles for Water Splitting Catalyzed by the Ru(II)−Pincer

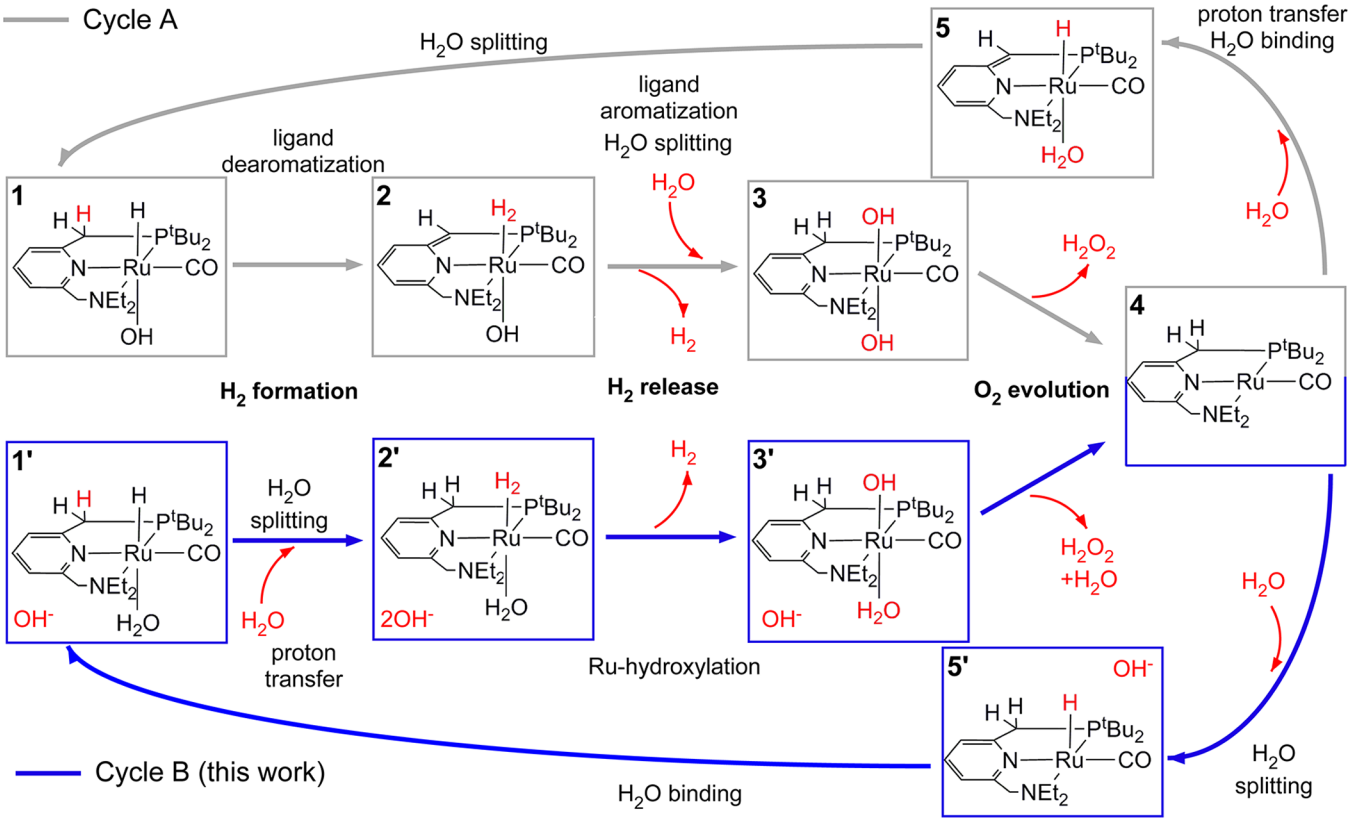

of the Ru atom does not change significantly in the **0** → **1**, **0** → **1′**, and **1** → **1′** transformations, thus suggesting that the Ru(II) center does not change its oxidation state.

3.3. H−H Bond Formation. The solvation analysis described above proposes that the relevant initial state for the catalytic cycle leading to H_2 and O_2 evolutions is complex **1′**. We note that the dihydrogen-bonded water molecule in the initial state **1′** is similar to the one proposed by Sandhya and Suresh.[19] In the following, we use CP MD and metadynamics to determine the mechanism of the H−H bond formation at the Ru center in explicit solvent. We consider and compare two possible mechanisms: M1, the one in which the H atom transfers from the C1 atom to the Ru center by assistance of a bridging water molecule; and M2, the one in which the H atom results from the splitting of a solvent water molecule nearby. The former involves ligand aromatization−dearomatization along the cycle and has been the subject of previous computational works (step **1** → **2** in cycle A of Scheme 2).[16,17] The latter is a prediction of our metadynamic simulations, turns out to have lower activation energy, and implies a catalytic cycle without aromatization−dearomatization of the PNN ligand.

We first sample the H−H bond formation mechanism M1 by biasing two collective variables (dashed lines in Figure 2a: (CV1) the Ru coordination number with respect to the hydrogen atom in the bridging water molecule and (CV2) the coordination number of the oxygen in the bridging water with respect to the hydrogen atom in the C1 site. The calculated (**1′** → **2**) free energy profile is displayed in Figure 2b (left panel) and clearly predicts a stepwise mechanism, at variance with the concerted mechanism identified on the basis of an implicit solvent description. This stepwise mechanism first involves the splitting of the bridging water molecule, which transfers a proton to the Ru center, forming the H_2 molecule and an hydroxide in solution (**1′** → **2′**). The second **2′** → **2** reaction step reforms the solvent water molecule by transferring a proton from the C1 site of the PNN ligand to the hydroxide in solution. The latter step is rate-limiting, with a calculated activation energy of 1.35 eV. Despite the mechanistic differences, stepwise vs concerted, this value is in good agreement with the previous estimates for mechanism M1, 1.26−1.46 eV,[16,17] showing that the deprotonation of the C1 site is rate-limiting in this reaction channel. Quite importantly, the metadynamics simulations clearly show that H−H bond formation via splitting of the solvent water molecule is definitely less energy-demanding than the deprotonation of the PNN ligand.

We now turn to the H−H bond formation mechanism M2, which we sample by two specific CVs (see Figure 2d): (CV1) the Ru coordination number with the H atom of the bridging water and (CV2) the coordination number between oxygen and hydrogen in the bridging water. The **1′** → **2′** free energy profile is displayed in Figure 2f. This rate-limiting step is repeated three times to obtain more accurate results. The calculated activation energies are 0.84, 1.01, and 0.77 eV, with an average of 0.87 (±0.1) eV, which are all considerably lower than the one for mechanism M1.

Our calculations show that the high energy barrier for the hydrogen formation step discussed in previous theoretical calculations can be attributed to the deprotonation of the PNN ligand (1.35 eV). The activation of a solvent water molecule and hydrogen transfer to Ru to form H_2, on the other hand, is considerably less energy-demanding (0.87 eV). These results suggest the possibility of an alternative reaction path for the

dx.doi.org/10.1021/cs300350b | ACS Catal. 2012, 2, 1500−1506

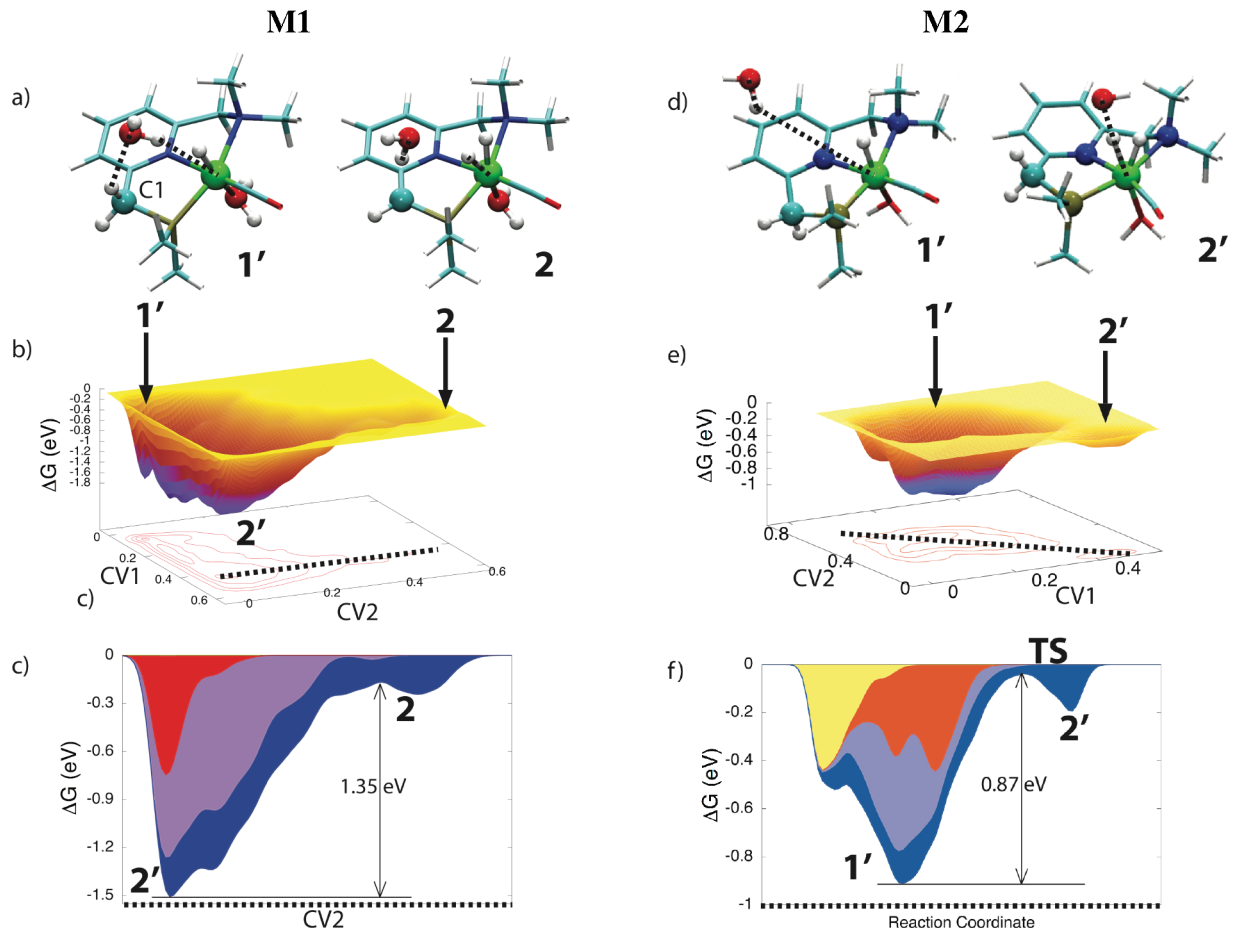

Figure 2. Comparison between the reaction mechanisms for H_2 formation via M1, deprotonating the C1 site of the PNN ligand with the assistance of a bridging water (left); or M2, splitting a solvent water molecule (right). (a, d) Representative configurations of the initial and final states taken from the molecular dynamics simulations. (b, e) Free energy surfaces as a function of the CVs defined as coordination numbers of Ru, O, and H (see dashed lines and text) used in the metadynamics. (c, f) 2D cuts of the free energy surface.

thermal evolution of H_2 that does not involve the aromatization−dearomatization of the catalyst during the cycle (see cycle B in Scheme 2)

CP MD simulations of the final state (**2′**) show that after H_2 desorption from the Ru center, the OH^- species present in solution quickly binds at the vacant site of the Ru atom (**2′** → **3′** in Scheme 2). This leads to the formation of trans aqua−hydroxo ligands at the Ru site. The high reactivity of the Ru center in the short-lived intermediate complex **2′** correlates with the large positive charge of the molecule relative to the other intermediates (Table S5 in the SI). The formation of complex **3′** through the binding of OH^- re-establishes the same overall charge of the initial state **1′**. During the **1′** → **3′** transformation, the computed charge of the Ru center increases by ∼0.2*e*.

As a further example of the complexity of these reactions in solution, we report a specific long-range process occurring during the simulation of the **1′** → **2′** step. The OH^- resulting from the proton transfer of the bridging water molecule to Ru is immediately saturated through proton transfer chains, leading to a quick diffusion of the OH^- in solution away from the Ru-pincer. Because of this, in the second step of the hydrogen formation reaction (**2′** → **2**), a proton is transferred from the methylene group to a water molecule rather than to a hydroxo. This leads to the formation of a hydronium that quickly reacts with the hydroxo present in solution, resulting in two water molecules. Clearly, these complex diffusions and reactions can only be captured through an explicit solvent simulation.

3.4. O_2 Evolution and Cycle Closure. In the catalytic cycle proposed by Kohl et al.,[14] the formation of O_2 is triggered by UV−vis irradiation through the formation of H_2O_2, which catalytically disproportionates into O_2 and water. This step has been modeled by Yang et al. considering, first, the OH and CO ligand exchange, leading to two neighboring OH groups that proceed to the formation of H_2O_2. The activated formation of H_2O_2 could involve two singlet−triplet crossings, promoted by the UV−vis radiation.[17] A similar mechanism could be at play also in the reaction path we propose (cycle B in Scheme 2), with the only difference that we now have an aqua instead of a hydroxo ligand. In this work, we do not investigate this radiation-promoted portion of the catalytic cycle. The final state of the O_2 evolution step proposed by Li et al. (complex **4** in Scheme 2) is, however, perfectly compatible also with the catalytic cycle we have identified so far. In the following, we propose the final steps that could close our cycle B (Scheme 2).

After the evolution of molecular oxygen, both sides of the Ru center are left unsaturated (**4**). Although we do not address explicitly the **3′** → **4** transformation, we note that it involves the largest relative variation of the Ru charge during the cycle (see Löwdin charge analysis in Table S5 of the SI). Overall, the Ru center becomes more negative by ∼0.5*e*. This variation likely results from the proton ligand, whose presence polarizes the

dx.doi.org/10.1021/cs300350b | *ACS Catal.* 2012, 2, 1500−1506

Ru−H bond, displacing charge density away from the Ru center. In catalytic cycle A, a H atom is transferred from the saturated carbon in the P side arm of the PNN ligand to the Ru center through a transition state while a solvent water molecule binds at the other side to form Ru complex **5**. Given the large activation free energy for the deprotonation of the C1 site in the PNN ligand, we explored the possibility that a proton from a solvent water molecule transfers directly to the metal center.

To investigate the process **4** → **5′**, we employed metadynamics simulations, biasing two collective variables: (CV1) the coordination number of Ru with respect to the hydrogen in the solvent water molecule and (CV2) the coordination number of this hydrogen with respect to the oxygen in the water molecule. In the initial state of this simulation (**4**), two solvent water molecules are coordinated to the Ru atom, with one of their hydrogen atoms pointing toward the Ru center (see Figure 3 a). Along the metadynamics run,

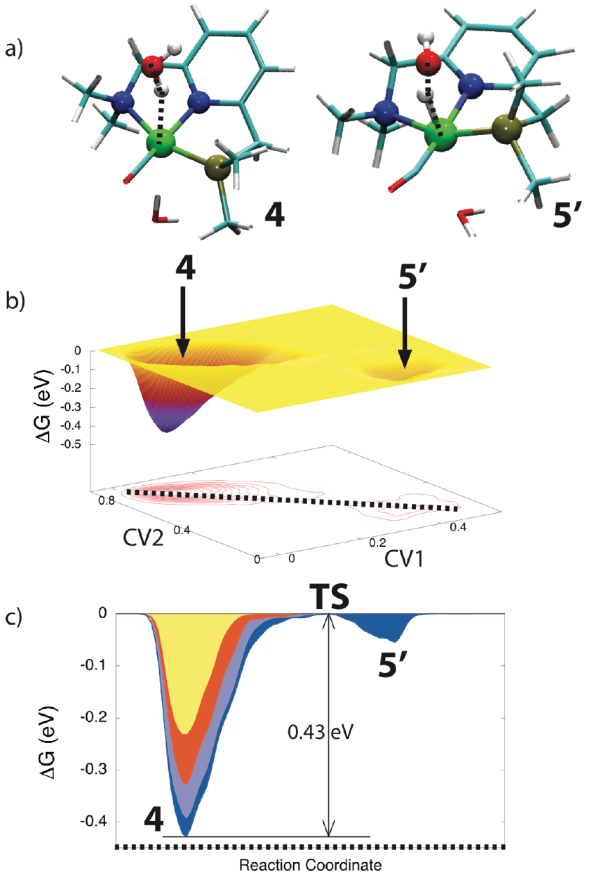

Figure 3. Reaction mechanism for hydride formation at the Ru center. (a) Representative configurations of the initial (**4**) and final (**5′**) states taken from the molecular dynamics simulations. (b) Free energy surface as a function of the CVs defined as the coordination number between Ru and H (CV1) and between O and H (CV2). (c) 2D cut of the free energy surface between **4** and **5′**. The activation energy is 0.43 eV.

one of the two water ligands splits and forms the Ru−H bond, and the second water ligand changes its binding geometry. In the final state (**5′**), the latter water molecule binds to the Ru atom through the lone pairs of the oxygen atom. This change in binding geometry is triggered by the transfer of a proton to the Ru atom. An analysis of the Löwdin charges of the initial and final states shows that upon the formation of the Ru−H bond, part of the electronic charge on the Ru atom (0.25*e*) is displaced toward the H atom. The polarization of the Ru−H bond leads a (relative) positive charge on the Ru atom, which favors the binding of the water ligand through the O atom rather than through the H atom.

We obtained for the **4** → **5′** step an activation energy of 0.43 eV (see Figure 3). This barrier is significantly lower than the one found for removing a proton from the saturated carbon in the P side arm of the PNN ligand (1.35 eV, as discussed in the previous section). These results suggest a new water splitting mechanism that does not involve ligand dearomatization (**4** → **5**), but the activation of a solvent water molecule and the proton transfer to the vacant site of the Ru center (**4** → **5′** in Scheme 2). Given the fact that during the **4** → **5′** step, while H is transferred to one of the two free sites at the Ru atom, a water molecule binds at the other site, we can picture **4** → **5′** → **1′** as a single step, taking the system back to the initial state and therefore closing the catalytic cycle (see Scheme 2).

4. CONCLUSIONS

This study demonstrates that ab initio simulations of complex reactions in solution may be very challenging, particularly when the solution enters directly into the catalytic cycle, such as in water oxidation reactions. We find that implicit and explicit modeling of the solvent yield very different reaction mechanisms for water splitting and H_2 evolution promoted by a Ru(II)-pincer catalyst. By means of DFT-based metadynamics simulations, we have identified a new reaction mechanism that rationalizes the function of this catalyst, which splits a solvent water molecule rather than a water ligand, and which does not undergo the previously proposed aromatization−dearomatization transition of the PNN ligand. The activation energy for the rate-limiting step of our mechanism is significantly lower (by ≈0.5 eV) than the one proposed in earlier works.[14,16,17]

The main difference between our reaction cycle and the one suggested in previous works concerns the aromatization−dearomatization of the PNN ligand through the protonation−deprotonation of its C site. In our catalytic cycle, this ligand of the Ru(II)-pincer always retains its aromatic character. In particular, by coupling metadynamics with an explicit solvent description, we show that the H−H bond formation is not a concerted mechanism, but a stepwise process that involves the participation of several water molecules, which mediate the transfer of hydroxide species in solution via proton chains. This demonstrates the active role played by the solvent in water oxidation reactions, which can be correctly captured only by simulations explicitly describing the solvent.

■ ASSOCIATED CONTENT

Supporting Information

Preliminary analysis in gas phase and computational details for metadynamics simulations. This material is available free of charge via the Internet at http://pubs.acs.org.

■ AUTHOR INFORMATION

Corresponding Author

*E-mail: fabris@sissa.it.

Notes

The authors declare no competing financial interest.

■ ACKNOWLEDGMENTS

The authors are grateful to Alessandro Laio for useful discussions about the metadynamics simulations, to Layla Martin-Samos for technical support for the PLUMED plug-in in Quantum ESPRESSO, and to Stefano Baroni for stimulating and supporting our interest in these topics. This work was partially supported by the EU through the FP7Marie Curie IRG Program (Project H2OSPLIT, Grant PIRG04-GA-2008-239199). CINECA is acknowledged for generous allocation of computational resources through the ISCRA scheme (Project HP10B8FMFJ).

■ REFERENCES

(1) Gray, H. *Nat. Chem.* **2009**, *1*, 7.
(2) Lewis, N. S.; Nocera, D. G. *Proc. Natl. Acad. Sci. U.S.A.* **2006**, *103*, 15729−15735.
(3) Balzani, V.; Credi, A.; Venturi, M. *ChemSusChem* **2008**, *1*, 26−58.
(4) Yamazaki, H.; Shouji, A.; Kajita, M.; Yagi, M. *Coord. Chem. Rev.* **2010**, *254*, 2483−2491.
(5) Sala, X.; Romero, I.; Rodrguez, M.; Escriche, L.; Llobet, A. *Angew. Chem., Int. Ed.* **2009**, *48*, 2842−2852.
(6) Armaroli, N.; Balzani, V. *Angew. Chem., Int. Ed.* **2006**, *46*, 52−66.
(7) Guskov, A.; Kern, J.; Gabdulkhakov, A.; Broser, M.; Zouni, A.; Saenger, W. *Nat. Struct. Mol. Biol.* **2009**, *16*, 334−342.
(8) Gersten, S.; Samuels, G.; Meyer, T. *J. Am. Chem. Soc.* **1982**, *104*, 4029−4030.
(9) Sartorel, A.; Carraro, M.; Scorrano, G.; Zorzi, R. D.; Geremia, S.; McDaniel, N. D.; Bernhard, S.; Bonchio, M. *J. Am. Chem. Soc.* **2008**, *130*, 5006−5007.
(10) Geletii, Y. V.; Botar, B.; Kögerler, P.; Hillesheim, D. A.; Musaev, D. G.; Hill, C. L. *Angew. Chem., Int. Ed.* **2008**, *47*, 3896−3899.
(11) McDaniel, N. D.; Coughlin, F. J.; Tinker, L. L.; Bernhard, S. *J. Am. Chem. Soc.* **2008**, *130*, 210−217.
(12) Zong, R.; Thummel, R. P. *J. Am. Chem. Soc.* **2005**, *127*, 12802−12803.
(13) Concepcion, J. J.; Jurss, J. W.; Templeton, J. L.; Meyer, T. J. *J. Am. Chem. Soc.* **2008**, *130*, 16462−16463.
(14) Kohl, S. W.; Weiner, L.; Schwartsburd, L.; Konstantinovski, L.; Shimon, L. J. W.; Ben-David, Y.; Iron, M. A.; Milstein, D. *Science* **2009**, *324*, 74−77.
(15) Murakami, M.; Hong, D.; Suenobu, T.; Yamaguchi, S.; Ogura, T.; Fukuzumi, S. *J. Am. Chem. Soc.* **2011**, *133*, 11605−11613.
(16) Li, J.; Shiota, Y.; Yoshizawa, K. *J. Am. Chem. Soc.* **2009**, *131*, 13584−13585.
(17) Yang, X.; Hall, M. *J. Am. Chem. Soc.* **2010**, *132*, 120−130.
(18) Chen, Y.; Fang, W. *J. Phys. Chem. A* **2010**, 1861−1870.
(19) Sandhya, K. S.; Suresh, C. H. *Organometallics* **2011**, *30*, 3888−3891.
(20) Kohn, W.; Sham, L. *Phys. Rev.* **1965**, *140*, A1133−A1138.
(21) Perdew, J.; Burke, K.; Ernzerhof, M. *Phys. Rev. Lett.* **1996**, *77*, 3865−3868.
(22) Vanderbilt, D. *Phys. Rev. B* **1990**, *41*, 7892−7895.
(23) Giannozzi, P.; Baroni, S.; Bonini, N.; Calandra, M.; Car, R.; Cavazzoni, C.; Ceresoli, D.; Chiarotti, G.; Cococcioni, M.; Dabo, I.; Dal Corso, A.; de Gironcoli, S.; Fabris, S.; Fratesi, G.; Gebauer, R.; Gerstmann, U.; Gougoussis, C.; Kokalj, A.; Lazzeri, M.; Martin-Samos, L.; Marzari, N.; Mauri, F.; Mazzarello, R.; Paolini, S.; Pasquarello, A.; Paulatto, L.; Sbraccia, C.; Scandolo, S.; Sclauzero, G.; Seitsonen, A. P.; Smogunov, A.; Umari, P.; Wentzcovitch, R. M. *J. Phys.: Condens. Matter* **2009**, *21*, 395502.
(24) Car, R.; Parrinello, M. *Phys. Rev. Lett.* **1985**, *55*, 2471−2474.
(25) Jorgensen, W.; Chandrasekhar, J.; Madura, J.; Impey, R.; Klein, M. *J. Chem. Phys.* **1983**, *79*, 926.
(26) Nose, S. *J. Chem. Phys.* **1984**, *81*, 511.
(27) Laio, A.; Parrinello, M. *Proc. Natl. Acad. Sci. U.S.A.* **2002**, *99*, 12562.
(28) Bonomi, M.; Branduardi, D.; Bussi, G.; Camilloni, C.; Provasi, D.; Raiteri, P.; Donadio, D.; Marinelli, F.; Pietrucci, F.; Broglia, R. *Comput. Phys. Commun.* **2009**, *180*, 1961−1972.